Keyhole Chemical Exchange Saturation Transfer

G. Varma[1], R. E. Lenkinski[1], and E. Vinogradov[1]
[1]Department of Radiology, Beth Israel Deaconess Medical Center, Harvard Medical School, Boston, MA, United States

Introduction: The contrast from chemical exchange saturation transfer (CEST) in MRI experiments has gained attention based on its inherent sensitivity to metabolic and physiological parameters as well as simple transition between an active and inactive ("on" and "off") state [1]. Many CEST experiments rely upon an analysis of Z-spectra, which in itself requires acquisitions following saturation at (on- and) off-resonance frequencies. However such sequential acquisition can be time-consuming and as such negate any potential benefit in acquiring images for CEST contrast. Time efficient techniques for capturing a dynamic change in contrast have been described based on the acquisition of the centre of k-space [2-4]. Keyhole experiments involve the use of a reference image combined with (dynamic) low-resolution data to produce images of supposed higher resolution that show an overall change in contrast [2]. Here, a keyhole technique is applied to CEST experiments. Images acquired at low resolution and reconstructed with a higher-resolution reference image using the keyhole technique are shown to retain the same CEST contrast and high resolution, at substantially shorter total acquisition time.

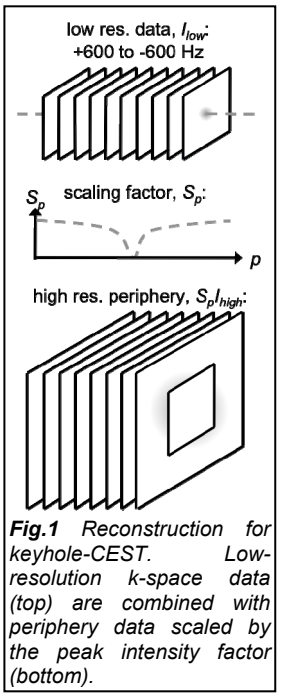

Fig.1 *Reconstruction for keyhole-CEST. Low-resolution k-space data (top) are combined with periphery data scaled by the peak intensity factor (bottom).*

Methods & Materials: This work concentrates on CEST contrast provided by –OH groups, such as those found in dextrose, glycogen (glycoCEST [5]) and on glycosaminoglycans in cartilage (gagCEST [6]). A phantom was prepared with samples of dextrose solution, 5% chondroitin sulphate (GAG) in saline, bovine nasal cartilage (BNC), and saline solution to serve as a control. Scans were carried out on a clinical 3T scanner using a transmit-receive knee coil. Saturation for CEST was achieved with a module carried out prior to a gradient-echo acquisition. The module consisted of 5 x 50ms gauss-shaped pulses with offsets in their frequency ranging from 600 to -600Hz in -50Hz increments for each sequential scan. Scan parameters were as follows: FOV = 12.8x12.8mm^2; matrix size = 64x64 (high resolution for comparison), 32x32 (low resolution for keyhole technique, N_{low}); and TE/TR = 4.6/500ms. Data were also collected without the preparatory module for normalisation of the CEST contrast. The high-resolution scan without saturation provided the periphery information for the keyhole technique. Phase correction (as used in homodyne reconstruction) was applied. To eliminate discontinuities in k-space, the data used for the periphery were scaled based on the peak amplitude of low-resolution data in k-space (Fig.1). For each offset in the Z-spectrum, *p*, the composite k-space image data $I_p(k)$ was created as: $I_p(k)=I_{low}(k)$ *for* $-N_{low}/2 \le k < N_{low}/2$ and $I_p(k)=S_pI_{high}(k)$ *otherwise*. Pixel-by-pixel Z-spectra were formed by normalizing the intensities to the reference intensity with no saturation. The B_0 inhomogeneities were taken into account by aligning the minimum of the Z-spectrum with 0 of the frequency axis. CEST maps were produced by integration of the Z-spectrum between +0.9 and +1.9ppm (where –OH groups resonate) and its subtraction from the value integrated over the same range upfield.

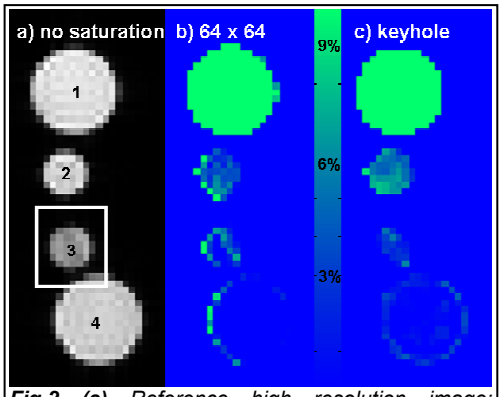

Fig.2 ***(a)*** *Reference high resolution image: 1=dextrose; 2=GAG; 3=BNC; and 4=saline. CEST maps formed by* ***(b)*** *data acquired with 64x64 matrix and* ***(c)*** *keyhole technique using 32x32 low-resolution data combined with high-frequency information from the reference.*

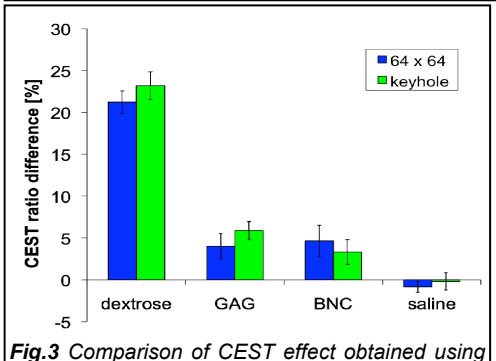

Fig.3 *Comparison of CEST effect obtained using high resolution and keyhole parameter maps.*

Results & Discussion: Figure 2 shows CEST maps formed using high-resolution data compared with that using the keyhole technique. Visual contrast is similar between the two, in particular from the homogenous samples of dextrose, GAG and saline solutions. Quantitative analysis of the two maps also shows little difference between the values extracted from regions of interest that encompass the samples (Fig. 3). Dextrose shows the greatest contrast based on the expected concentration of –OH groups. The saline sample serves as a control and shows close to zero contrast despite saturation relatively close to the on-resonance pool. BNC values are similar to those from the GAG solution. Contrast from the piece of BNC is readily observed in the high-resolution images acquired with saturation applied at a frequency within the +0.9 to +1.9ppm range (Fig.4a). Images reconstructed with the keyhole technique also show BNC and allow contrast visualization from saturation of the BNC (Fig. 4b-c). At the same time, the low-resolution image alone does not delineate between BNC and surrounding saline (Fig.4d). This result shows promise for looking at the CEST effect from relatively thin structures, such as articular cartilage. The use of techniques similar to keyhole that provide a dynamic update of some higher frequency parts in k-space combined with the acquisition for CEST might offer further contrast improvement [3,4].

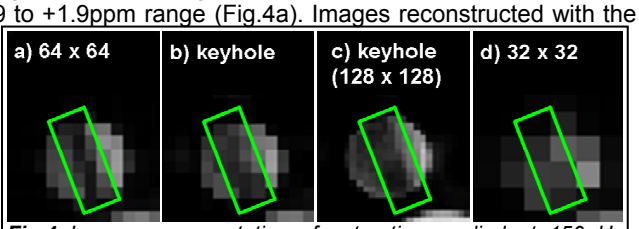

Fig.4 *Images representative of saturation applied at 150 Hz obtained* ***(a)*** *at high resolution,* ***(b)*** *from the keyhole technique,* ***(c)*** *from the keyhole technique using a 128 x128 reference image, and* ***(d)*** *only using the low-resolution data.*

Conclusions: The keyhole technique has been combined with Z-spectra acquisition to show CEST contrast from –OH groups on a clinical scanner. The CEST effect is comparable to that obtained from high-resolution data, at about half of the total scan time. Therefore this, or other similar techniques, can be used to generate Z-spectra with significant reduction in scan time.

References: [1] Ward et al. JMR 2000:79-87. [2] van Vaals et al. JMRI 1993:671-5. [3] Doyle et al. MRM 1995:163-70. [4] Korosec et al. MRM 1996:345-51. [5] van Zijl et al. Proc Natl Acad Sci 2007:4359-64. [6] Ling et al. Proc Natl Acad Sci 2008:2266-70.